University of California, San Diego

UCSD-CER-05-09

"Engineering Analysis of He Retention and Release in Porous W Armor"

A. René Raffray

27 September 2005

Center for Energy Research
University of California, San Diego
9500 Gilman Drive
La Jolla, CA 92093-0420

Subcontracting Work Performed by UCSD for Plasma Processes Inc. as Part of DoE STTR Phase II Grant "Engineered Tungsten Armor for IFE Dry Chamber Walls"

Interim Report

September 27, 2005

A. René Raffray

I. Background

The chamber wall armor faces demanding conditions in inertial fusion energy (IFE) chambers. IFE operation is cyclic in nature (~1-10 Hz) and following each microexplosion, the chamber wall is subjected to a burst of photons, energetic particles and neutrons. Key issues include; (i) chamber clearing to ensure that after each shot the chamber returns to a quiescent state in preparation for the target injection and the firing of the driver for the subsequent shot, and (ii) armor lifetime which requires the armor to accommodate the cyclic energy deposition while providing the required lifetime. These requirements are major factors in evolving the choice of armor configuration and material. Dry wall options are particularly amenable to laser IFE and the candidate armor material must provide high temperature resistance and accommodate the operating conditions with minimal erosion. Refractory metals such as tungsten can provide these capabilities and accommodate the high energy deposition [1]. However, a major concern is the possible accumulation of helium from ion implantation. Helium migration in tungsten is slow and the concern is that a build-up of helium could result in local armor failure.

A possible solution is to minimize the migration distance of helium in the tungsten structure which coupled with the high temperature of operation could help implanted helium migrate back to the chamber. A very fine tungsten grain structure (~nanometers) might help in achieving this by providing a very short distance for helium to reach the

grain boundary where diffusion should be faster. In addition, if nano-sized interconnected porosity could be incorporated in the structure, it would be very beneficial providing a path of least resistance to helium migration back to the chamber. An important consideration is that development of this innovative tungsten structure should also be done while maintaining the required high heat flux and high temperature capability of the armor.

II. Proposed Configuration

As shown in Fig. 1, the overall configuration envisaged for this application consists of a porous W layer over a fully dense W layer which is attached to a ferritic steel structure representing the first wall of an IFE chamber. PPI proposes to use a vacuum plasma spray forming technique to manufacture such a layered structure with a functional gradient when transitioning from porous to fully dense W as well as when transitioning from fully dense W to ferritic steel.

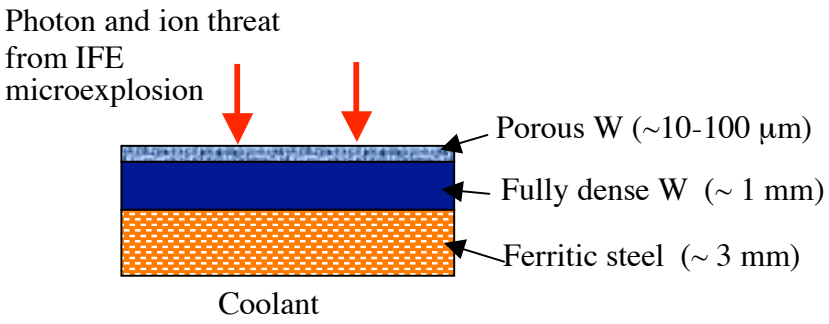

Fig. 1 Schematic of engineered W armor/first wall configuration

III. Phase I Summary

We have worked together with PPI as part of Phase I of this grant in scoping out the W microstructure that would potentially provide both a short diffusion path for release of He

and adequate thermal performance under the ion and photon energy deposition [1]. A scoping analysis was done for a thin porous W armor layer on top of a fully dense W layer which would be attached to a ferritic steel wall in an IFE chamber. As summarized in Fig. 2, the results indicated that the maximum armor temperature increases appreciably with increasing porosity but not with porous region thickness (past the ion penetration depth which is <10μm). There are two porosity-dependent, competing mechanisms affecting the W porous region temperature rise: (i) increasing the porosity lowers the maximum energy deposition while spreading it spatially which tends to reduce the maximum W armor temperature; and (ii) increasing the porosity lowers the thermal conductivity of the porous region which tends to result in higher armor temperature. Of these two, the later seems to have a stronger effect judging from the results in Figure 2. Thus, it seems important to minimize the porosity of the porous region (< ≈20% if possible) but there seems to be flexibility in setting its thickness. The porous region might also reduce peak thermal stresses on the armor and allow for higher maximum temperature limits.

Scoping studies of helium migration were also performed. This is a complex process involving a number of mechanisms. For simplicity, initial estimates were based on bulk diffusion with the understanding that other mechanisms such as trapping would tend to slow down the He migration process. The following diffusion coefficient for He in W was used to estimate the porous microstructure dimension for He to diffuse out as a function of temperature and time.

$$D\ (m^2/s) = D_0 \exp(-E_{Dif}/kT) \quad (1)$$

From Wagner and Seidman [2]:

$$D_0 = 4.7 \times 10^{-7}\ m^2/s \text{ and } E_{Dif} = 0.28\ eV \quad (2)$$

For a temperature of ≈1000-1500K over a time of 0.1 s, the characteristic He diffusion dimension ≈10-50 nm. Higher temperature would help but shorter times would hurt. From these initial results, the goal should be to have interconnected porosity and

microstructure of dimension ≈10-100 nm. These results have to be confirmed through more detailed modeling and experiments as part of Phase II. This has been the focus of our initial effort during Phase II and is summarized in the subsequent sections.

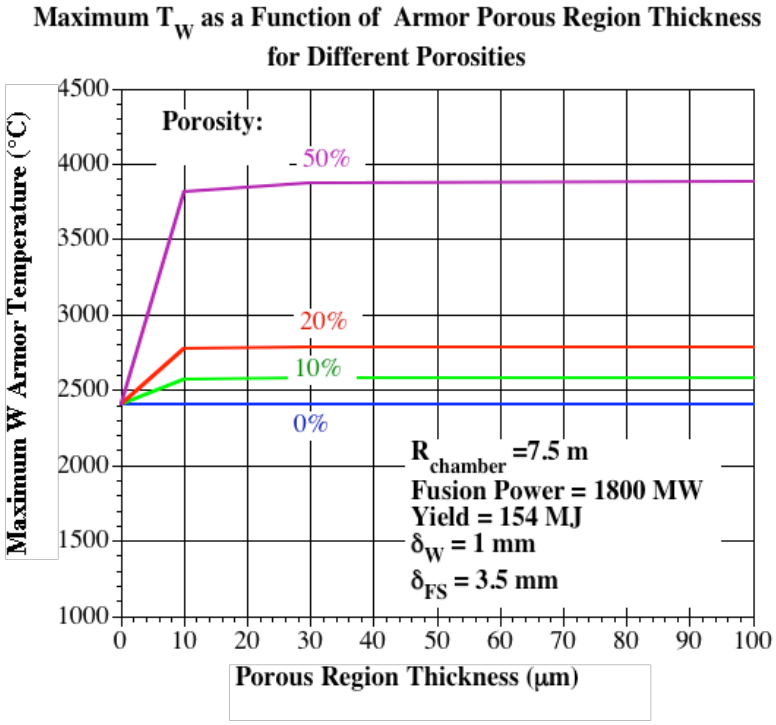

Figure 2 Maximum W armor temperature as a function of the porous region thickness for different porosities of this region, for the 154 MJ direct drive target. The assumed thicknesses of the fully dense W layer and of the ferritic steel structure are 1 mm and 3.5 mm, respectively and the assumed coolant temperature is 572°C [1].

IV. Phase II Effort

IV.1 Cyclic He Implantation and Temperature Profiles

The initial effort focused on trying to better understand the behavior of He implanted in W and to model experimental data in order to try to extrapolate to IFE prototypical conditions and obtain a better understanding of the He retention in the engineered W armor based on its characteristic microstructure dimension.

The He concentration after each shot can be estimated based on the total number of ions produced, the chamber surface are and the implantation depth. Figure 3 shows the spectra for the DD 154 MJ target [3,4]. The total number of He ions produced per shot can be estimated from the spectra data to be about $3x10^{19}$[3]. Currently, a higher yield target is being considered in HAPL (350 MJ) and the number of He ions will then be about $6.8x10^{19}$ just by simple scaling.

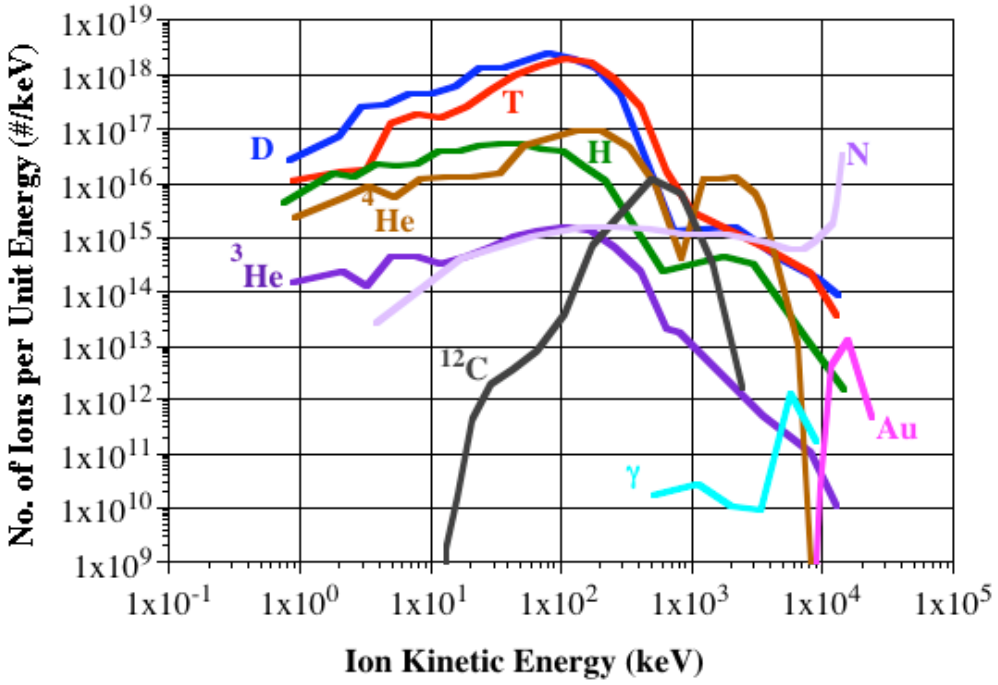

Figure 3 Fast ion and debris ion spectra from NRL 154 MJ direct drive target [3,4]

From Fig. 3, the energy of the He ions range from about 1 keV to a few MeV's. From SRIM [5], the projected range of He in W is about 1.5 nm at 1 keV, 23.8 nm at 10 keV, 217 nm at 100 keV, 1.41 μm at 1 MeV and 6.14 μm at 4 MeV. It seems reasonable to assume an average value of about 1.5 μm in estimating a representative He concentration after each micro-explosion. For a chamber size of about 10.5 m for the case of a chamber without a protective gas [4], the resulting concentration of implanted He ions in the W armor is ~ $3.2x10^{22}$ atoms/m^3.

Following each He implantation cycle, the armor will undergo a cyclic temperature increase based on the photon and ion energy deposition, as typically shown in Fig. 4 for an example case with the current reference 350 MJ target. These results were obtained from the RACLETTE-IFE code [6,7]. The key is to be able to understand the He behavior under such cyclic implantation and temperature profiles.

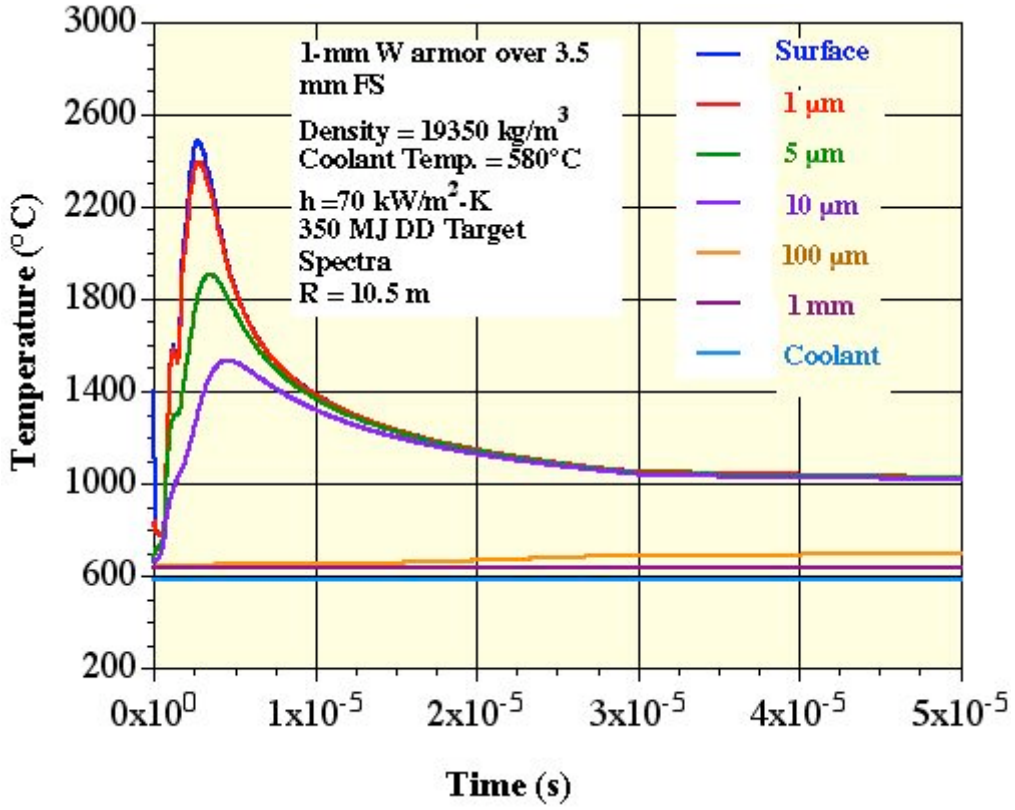

Figure 4. Example temperature history at different locations in a 1 mm W armor over a 2.5 mm ferritic steel substrate cooled by a 580°C coolant based on the estimated power deposition for a 350 MJ direct drive target spectra and assuming a chamber radius of 10.5 m and no protective gas in the chamber.

IV.2 Processes Affecting He Behavior in W

The initial effort focused on trying to better understand the behavior of He implanted in W. Through a literature search, a better picture emerged of the overall processes involved. Due to their high heat of solution, inert-gas atoms are essentially insoluble in most solids. Gas atom can then lead to gas-atom precipitation, bubble formation and

ultimately to destruction of the material. Helium atoms in a metal may occupy either substitutional or interstitial sites. As interstitials, they are very mobile, but they will be trapped at lattice vacancies, impurities, and vacancy-impurity complexes [8]. The following activation energies were estimated for different He processes in tungsten [8,9]:

Helium formation energy:	5.47 eV	(3)
Helium migration energy:	0.24 eV	
He vacancy binding energy:	4.15 eV	
He vacancy dissociation energy:	4.39 eV	

It seems reasonable to characterize the behavior of helium in tungsten through the major processes shown in Fig. 5.

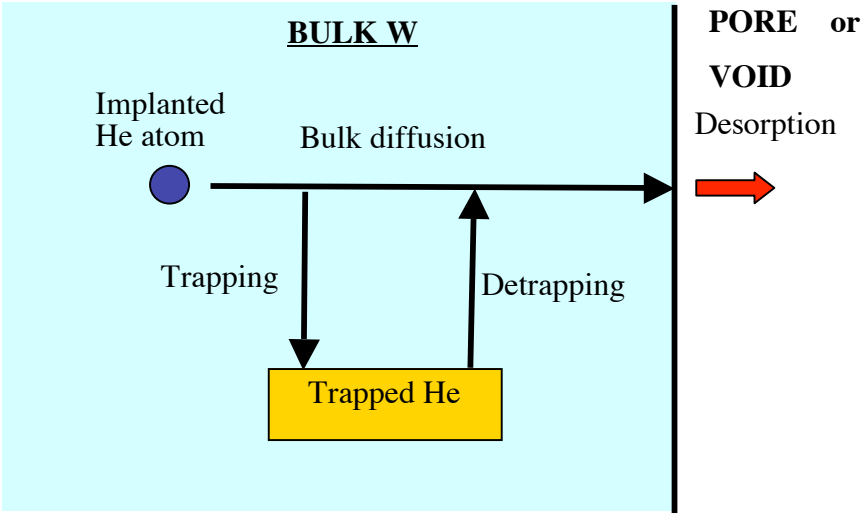

Figure 5 Schematic representation of some of the major processes affecting He behavior in W.

The implanted He would diffuse through the bulk of the W and then be trapped in vacancy, defect or other trapping sites. If sufficient energy is available the trapped atom can be detrapped and diffuse further through W. Eventually at the W surface interface, He would desorb to the surrounding atmosphere. These overall processes might include more than one mechanism. For example different trapping processes might be in play.

All these processes are governed by activation energies which might also change with the He concentration. For example the binding energy would change with increasing population of trapped He. The formation of He bubbles also mean a different set of energies as opposed to atomic He. The material thermo-mechanical conditions would also impact the overall He behavior. For example, the implantation of He at IFE energies would result in defects or high dpa's (thousands). However, the high temperature following the implantation (see Fig. 4) would tend to anneal out these defects except for those occupied by He already. An effort is underway to develop a detailed model for He behavior in W (HEROS) [10]. However, this is highly challenging due to the number of unknown parameters that need to be defined and characterized and the difficulty of validating such a model due to the scarcity of IFE relevant experimental data which are currently available.

IV.3 HAPL Experimental Effort on He Behavior in Tungsten Under IFE Conditions

As part of the HAPL program, there are experimental studies focused on investigating the helium retention and surface blistering characteristics of tungsten with regard to helium dose and temperature (as well as the effect of deuterons). Ultimately, the goal is to determine if helium retention can be mitigated by the pulsed nature of the helium implantation in combination with the high temperature thermal spikes within the IFE reactor. The experimental activities are performed through a collaboration between the University of North Carolina (UNC) and ORNL (high base temperature, ~850°V, high energy, ~1.3 MeV, pulsed implantation and anneals at 2000°C over ~ 1000 cycles to fluences of ~10^{20} He/m^2)[11] and, separately, by the University of Wisconsin in Madison (high temperature, ~800° or more, modest energy, ~10-100 keV, pulsed implantation to fluences of ~10^{22} He/m^2)[12].

Recent results from the UNC/ORNL effort suggest that certain conditions may mitigate the effect of He trapping and bubble formation. Less trapping of helium was observed in single crystal tungsten under certain conditions when compared to polycrystalline tungsten from the He implantation and anneal study, whose conditions and results are

summarized in Figures 6 and 7, respectively [13]. More importantly, the results indicate that He retention decreases drastically when a given helium dose is spread over an increasing number of pulses, each one followed by W annealing to 2000°C, to the extent that there would be no He retention below a certain He dose per pulse. For example, from Fig. 7, for single crystal tungsten, this threshold would be of the order of 10^{16} ions/m^2 per shot. For the IFE case of a 350 MJ target in a 10.5 m chamber, this threshold is still too high as the He dose per shot would be ~5x10^{16} ions/m^2. However, for the IFE case the W armor surface temperature would be closer to 2400°C which would significantly increase the helium mobility and, thus, should also significantly increase the per-shot threshold at which helium begins to accumulate.

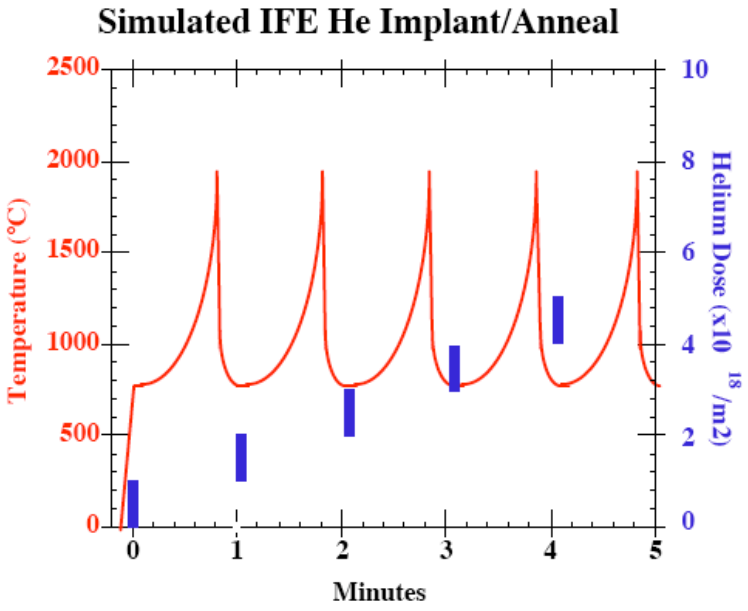

Figure 6 He dose implantation and temperature anneals for experiments simulating He retention in tungsten under IFE conditions [13].

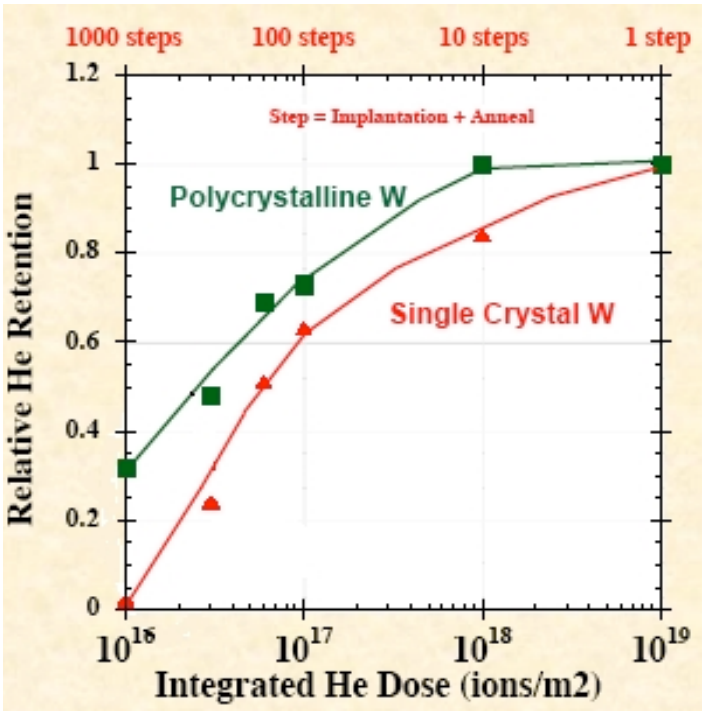

Figure 7 Relative He retention in polycrystalline and single crystal W samples as a function of He dose per cycle for different number of pulses based on He implantation and temperature anneals illustrated in Fig.6 [13].

IV.4 Modeling the Experimental Results

Development of a detailed model for He retention in W is quite complex and definition of input parameters very challenging due to the lack of information for IFE-relevant conditions. It was decided for the scope of this work and in order to obtain some preliminary insight on the application of experimental results to the IFE conditions to derive an effective diffusion coefficient which would be based on the combination of processes and which would be applicable for the same range of conditions. It is clear that in doing so the activation energy derived from the experiment would not be that of bulk diffusion but of the rate-controlling mechanism much probably some form of trapping/ detrapping mechanisms. The diffusion equation was solved assuming symmetry boundary condition at x=0 and assuming fast desorption at the surface (C = 0 at x = δ), as shown in Fig. 8

$$\frac{\partial C_g(x,t)}{\partial t} = D(T)\left(\frac{\partial^2 C_g(x,t)}{\partial t^2}\right) \qquad (4)$$

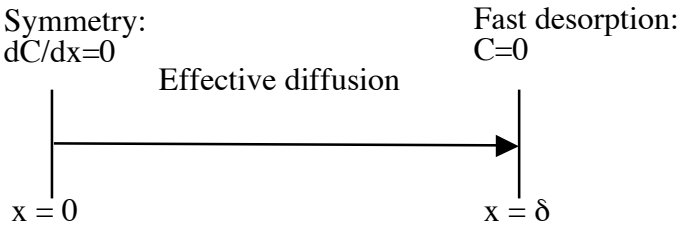

Figure 8 Simple effective diffusion model

The pre-exponential constant for diffusion was set to the same value as for the bulk diffusion case shown in eq. (2), D_0 = 4.7 x 10-7 m^2/s. The diffusion length, δ, was set at 1.5 μm consistent with the implantation depth of He ions with energies ~ 1 MeV energy (used in the experiment). The calculations proceeded by assuming a step He implantation concentration (in atoms/m^3 based on the dose and the implantation depth) as source term followed by diffusion over the temperature history shown in Fig. 5 for the anneal process. This procedure is repeated over the given number of cycles with the aim of finding the activation energy of the effective diffusion coefficient ($E_{eff,diff}$) which would yield the final retention value measured experimentally in each case (i.e. for 1, 10, 100, 167, 333 and 1000 cycles). The interesting observation is that, based on the results, for all results quasi steady state has not been reached yet, as illustrated for the 1000 cycles case for the polycrystalline material shown in Fig. 8.

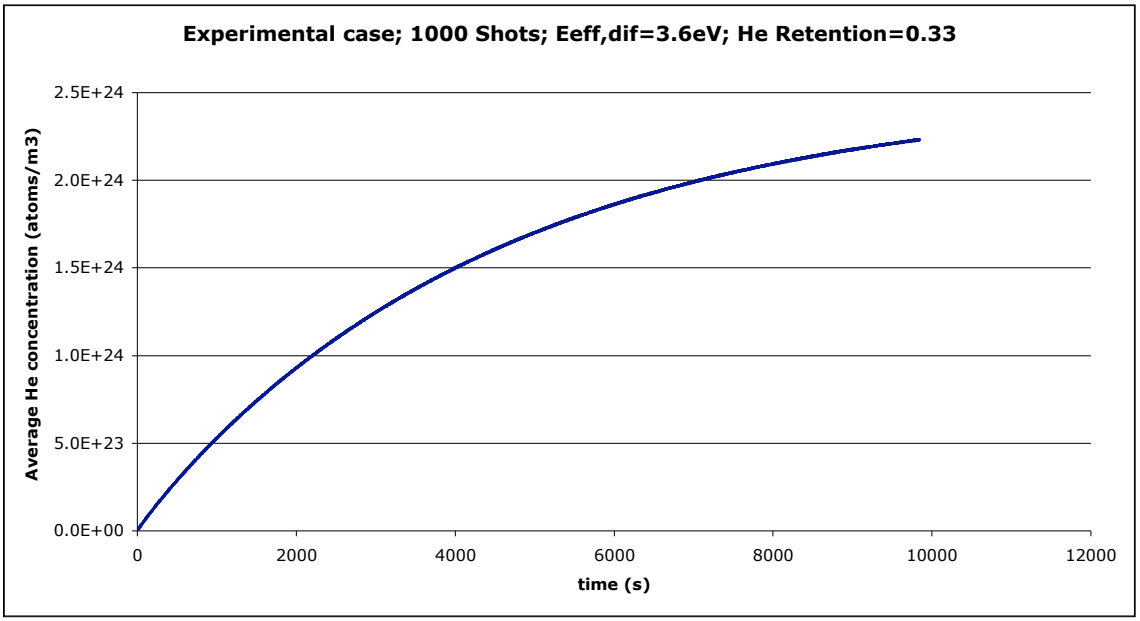

Figure 8 He concentration in polycrystalline W as a function of time for the case with 1000 shots and 0.33 retention in the end ($E_{eff,diff}$ = 3.6 eV).

The overall results are summarized in Table 1 and Figure 9. A possible interpretation of the results is given as follows.

The basic assumption is that trapping in general increases with the He irradiation dose or concentration which creates sites through dpa's and formation of vacancies (followed by an anneal of the unoccupied trapped sites during the ensuing temperature transient). At very low dose, only a few trapping sites are activated by the irradiation and the helium transport should be governed by bulk diffusion (with an activation energy of ~0.24-0.28eV from eqs. (2) and (3)). As the dose per cycle increases, an increasing number of trapping sites are formed or activated (e.g. through He ion irradiation induced dpa's and vacancy formation) and the activation energy increases. It seems that there is a near-threshold of He dose at which the activation energy increases rapidly to about 3.3-3.6 eV and stays at this value over a dose of ~$2x10^{16}$ to ~ $5x10^{18}$ ions/m^2 for single crystal W and about ~$5x10^{15}$ to ~ $5x10^{17}$ ions/m^2 for polycrystalline. Above this range, the activation energy increases rapidly to ~ 4.2-4.8 eV, indicating an increase in trapping perhaps due to He build up in vacancies (the vacancy dissociation energy is ~4.4 eV from eq. (3)).

Overall the dependence of activation energy with dose is about the same for single crystal and polycrystalline W except that it is shifted to lower doses for the latter case.

Table 1 Summary of results from modeling experimental data

No. of cycles	Dose per cycle (atoms/m^2)	Approx. He implanted concentrat. per cycle (atoms/m^3)	He retention (normalized to total amount of implanted He)	$E_{eff,diff}$ (eV)
Single Crystal W				
1	10^{19}	$6.67x10^{24}$	1	~4.2-4.4
10	10^{18}	$6.67x10^{23}$	0.83	3.30
100	10^{17}	$6.67x10^{22}$	0.63	3.42
167	$6x10^{16}$	$4.0x10^{22}$	0.51	3.41
333	$3x10^{16}$	$2.0x10^{22}$	0.23	3.33
1000	10^{16}	$6.67x10^{21}$	0.0001	2.40
Polycrystalline W				
1	10^{19}	$6.67x10^{24}$	1	~4.4-4.8
10	10^{18}	$6.67x10^{23}$	1	~4.4-4.8
100	10^{17}	$6.67x10^{22}$	0.73	3.53
167	$6x10^{16}$	$4.0x10^{22}$	0.69	3.57
333	$3x10^{16}$	$2.0x10^{22}$	0.48	3.51
1000	10^{16}	$6.67x10^{21}$	0.33	3.60

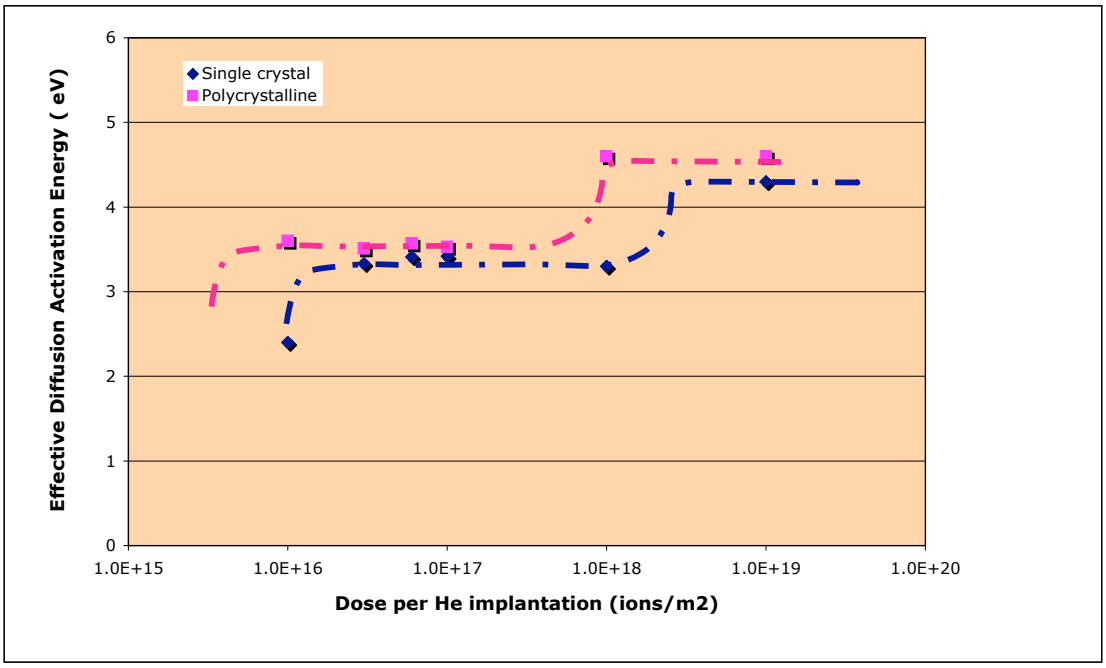

Figure 9 Effective diffusion activation energy required to reproduce the experimental results for single crystal and polycrystalline W. The curve fit has been drawn to suggest a possible variation of the activation energy with the He dose (or concentration).

IV. 5 Simulating the IFE Case

Results from the modeling analysis of the experimental results can be applied to help shed some light on the IFE case. For example if one assumes that the activation energy of the effective diffusion process is a function of the He implantation conditions (dose, energy). The He ions in the IFE case have a wide range of energies and penetration depths whereas the experiments were performed with mono-energetic ions (~1 MeV). As an initial approximation, it is assumed that the trapping behavior (and activation energy) is a function of the implanted He concentration. For the IFE case, the total He implanted dose per shot is ~5 x 10^{16} atoms/m^2 (with a concentration per shot of ~ 3.2x10^{22} atoms/m^3 for an assumed 1.5 μm average penetration depth (see section IV.1). When comparing this to the results in Fig. 9, the activation energy for effective diffusion should be ~3.38

eV for single crystal W, and ~ 3.52 eV for polycrystalline W, which are the values used for simulating the IFE case. The calculations were performed over 10,000 cycles (over a 0.2 s period assuming a rep. rate of 5) with the He implantation concentration followed by the temperature anneal (similar to the armor surface temperature history shown in Fig. 4). The polycrystalline case is more representative of the porous W armor microstructure and the results for that case (with an effective diffusion activation energy of 3.52 eV) are shown graphically in Fig. 10 for different diffusion distances representative of the characteristic dimension of porous W.

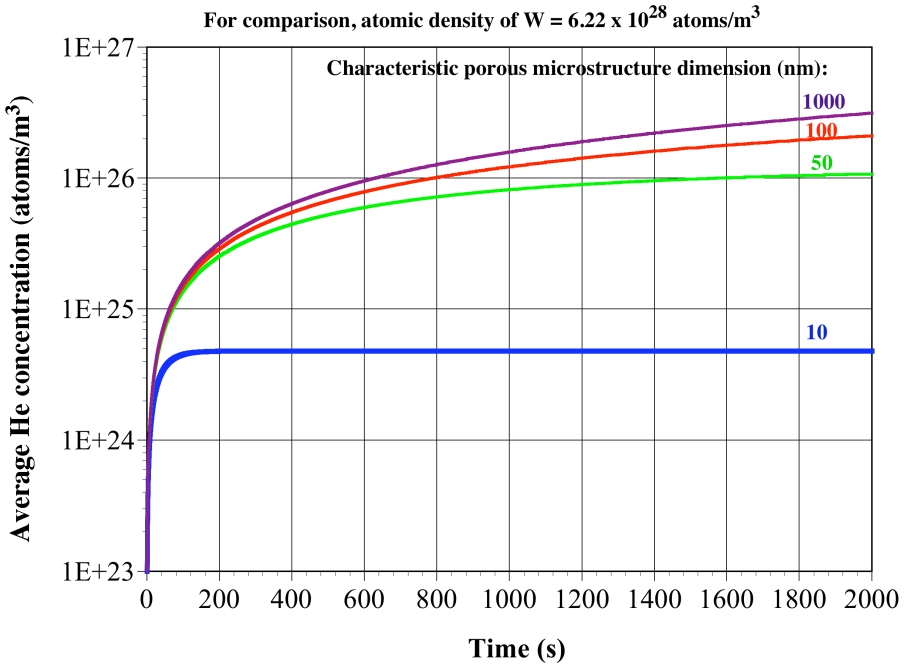

Figure 10 He concentration in the IFE W armor as a function of time for different characteristic porous microstructure dimensions and for an activation energy of 3.52 eV for effective diffusion.

It is interesting to note that quasi steady state was achieved for the cases with characteristic dimensions of 10 and 50 nm, respectively. However, for the 100 and 1000 nm cases, quasi steady state has not been reached yet.

The estimated maximum He concentration results (as absolute values and relative to the W concentration of 6.22 x 10^{28} atoms/m^3) are listed in Table 2 for effective diffusion activation energies corresponding to both the single crystal and polycrystalline cases. The

He concentration for the single crystal case ($E_{eff,diff}$=3.38 eV) is about half that of the polycrystalline case ($E_{eff,diff}$=3.52 eV) which gives a measure of the sensitivity of the results to small changes in the effective diffusion activation energy. The key question is what atomic fraction of He in W would be acceptable for the W armor to provide the required lifetime. In an earlier presentation, it was suggested that the critical ion/atom concentration for a blister to exfoliate is about 15 at.% for He in W [14]. This suggests that the microstructure characteristic dimension could be between 0.1 and 1 μm (the corresponding atomic fraction of He retained being ~0.4-0.8 in the latter case). However, given the included assumptions and simplifications in the modeling results presented here and in the absence of more prototypical experimental results, it seems reasonable to maintain the porous tungsten microstructure in the range 50-100nm, which would reduce the He retention to about 0.1-0.8%. A 10 nm microstructure, if it could be made, would be even better with a fractional He retention of only about 4 $x10^{-5}$ to 8 $x10^{-5}$ (normalized to the W atomic concentration).

In addition, as indicative of the results for cases with lower He ion doses corresponding for example to a lower yield target or to a larger chamber, example results for $E_{eff,diff}$=2.4 eV are also included in Table 2 (corresponding to doses $<10^{16}$ ions/m^2 per shot from Fig.9). Clearly, the He retention is much reduced (by about two orders of magnitude compared to the other cases) indicating that it would be very desirable to operate at ion doses below the lower ion dose threshold indicated in Fig. 9. This threshold seems to be ~10^{16} ions/m^2 based on these initial experimental results. Future effort is needed to confirm these results and also to better characterize and understand the material form dependence of this threshold (a factor of five increase would bring it very close to the current IFE case).

Table 2 Summary of results from modeling He retention in the IFE armor

Microstructure dimension (nm)	Maximum He concentration (atoms/m^3)	He retention concentration (normalized to atomic concentration of W = 6.22 x 10^{28} atoms/m^3)
Single Crystal W $E_{eff,diff}$=3.38 eV		
10	~2.6x10^{24}	~4.2x10^{-5}
50	*~6.5x10^{25} (estimated)*	~1.1 x 10^{-3}
100	*~2.6x10^{26} (estimated)*	~4.2x10^{-3}
1000	*~2.6x10^{28} (estimated)*	~0.42
Polycrystalline W $E_{eff,diff}$=3.52 eV		
10	~4.8x10^{24}	~7.7x10^{-5}
50	*~1.2x10^{26}(estimated)*	~1.9 x 10^{-3}
100	*~4.8x10^{26}(estimated)*	~7.7x10^{-3}
1000	*~4.8x10^{28}(estimated)*	~0.77
Example low ion flux case $E_{eff,diff}$=2.4 eV		
10	~4x10^{22}	~6x10^{-7}
50	~9x10^{23}	~1.5x10^{-5}
100	~4x10^{24}	~6x10^{-5}
1000	*~4x10^{26} (estimated)*	*~6x10^{-3}*

V. Summary and Conclusions

- Our initial effort during Phase II has focused on trying to understand recent experimental results on He retention following cycles of He ion implantation and temperature anneals. Many processes are involved and it is quite complex and difficult to develop a detailed model in particular since not much information is available on IFE relevant input parameters. We decided instead to assume an effective diffusion coefficient whose activation energy would depend on the governing mechanism under local conditions.

- The basic assumption is that trapping in general increases with the He irradiation dose or concentration which creates sites through dpa's and formation of vacancies (followed by an anneal of the unoccupied trapped sites during the ensuing temperature transient). At very low dose, the helium transport should be governed by bulk diffusion. As the dose per cycle increases, an increasing number of trapping sites are formed or activated (e.g. through He ion irradiation induced dpa's and vacancy formation) and the activation energy increases. It seems that there is a near-threshold of He dose at which the activation energy increases rapidly to about 3.3-3.6 eV and stays at this value over a dose of ~$2x10^{16}$ to ~$5x10^{18}$ ions/m^2 for single crystal W and about ~$5x10^{15}$ to ~ $5x10^{17}$ ions/m^2 for polycrystalline. Above this range, the activation energy increases rapidly to ~4.2-4.8 eV, indicating an increase in trapping perhaps due to He build up in vacancies (the vacancy dissociation energy is ~4.4 eV from eq. (3)). Overall the dependence of activation energy with dose is about the same for single crystal and polycrystalline W except that it is shifted to lower doses for the latter case.

- The activation energy results from the analysis of the experimental data was used to predict He retention for an IFE case. The He dose (or concentration) per cycle in the IFE case would correspond to an activation energy of ~3.38 eV for the single crystal

case and ~3.52 eV for the polycrystalline case from the experimental analysis; these values were used in the simulation.

- It is interesting to note that quasi steady state was achieved for the cases with characteristic dimensions of 10 and 50 nm, respectively. However, for the 100 nm and 1000 nm cases, quasi steady state was not reached yet.

- The key question is what atomic fraction of He in W would be acceptable for the W armor to provide the required lifetime. Ref. [14] suggests that the critical ion/atom concentration for a blister to exfoliate is about 15 at.% for He in W. This means that the microstructure characteristic dimension could be between 0.1 and 1 μm (the corresponding atomic fraction of He retained being ~0.4-0.8 in the latter case). However, given the included assumptions and simplifications in the modeling results presented here and in the absence of more prototypical experimental results, it seems reasonable to maintain the porous tungsten microstructure in the range 50-100nm, which would reduce the He retention to about 0.1-0.8%. A 10 nm microstructure, if it could be made, would be even better with a fractional He retention of only about 4 x 10^{-5} to 8 x10^{-5} (normalized to the W atomic concentration).

- In addition, as indicative of the results for cases with lower He ion doses corresponding for example to a lower yield target or to a larger chamber, cases for $E_{eff,diff}$=2.4 eV were also run. Clearly, the He retention is much reduced (by about two orders of magnitude compared to the other cases) indicating that it would be very desirable to operate at ion doses below the lower ion dose threshold indicated in Fig. 9. This threshold seems to be ~10^{16} ions/m^2 based on these initial experimental results. Future effort is needed to confirm these results and also to better characterize and understand the material form dependence of this threshold (a factor of five increase would bring it very close to the current IFE case).

- The results tend to confirm the results from Phase I suggesting interconnected porosity and microstructure of dimension ≈10-100 nm as a goal for implanted helium release.

- It is important to realize that these results are based on simplifying assumptions and simplifications. They provide some insight as to the He retention processes and the W microstructure dimension that would help maintain helium retention to an acceptable level. However, the results and related observations must be verified by experiments.

- It is hoped that such He retention experiments will be performed in the near future on the engineered W and the goal of the next phase of this study will be to help in pre- and post-experimental analysis of such experiments.

- It is also expected that thermo-mechanical testing of the engineered W armor will be carried out in the various HAPL-related test facilities (ions at RHEPP, SNL; X-rays at XAPPER, LLNL; and laser at Dragonfire). The next phase of this study will also include pre- and post-experimental analysis of these experiments with the goal in the end to identify an optimal porous engineered W armor configuration that can be manufactured by PPI and that would provide for acceptably low He retention and acceptable armor lifetime.

References

1. A.R. Raffray and J. Pulsifer, Final Report for DoE STTR Phase-I Subcontract from Plasma Processes Inc. to UCSD on"Engineered Tungsten Armor for IFE Dry Chamber Walls, "April 12, 2004

2. A. Wagner and D. N. Seidman, Phys. Rev. Letter **42**, 515 (1979)

3. Available at: http://aries.ucsd.edu/HAPL/DOCS/reftarget.html

4. A. R. Raffray, et al., Progress Towards Realization of a Laser IFE Solid Wall Chamber," invited presentation at ISFNT-7, Japan, 2005, to appear in Fusion Engineering & Design.

5. Available at http://www.srim.org/

6. A. René Raffray, et al., and the ARIES Team, "Dry Wall Survival Under IFE Conditions," accepted for publication in Fusion Engineering & Design, 2004

7. A. R. Raffray, and G. Federici, "RACLETTE: A Model for Evaluating the Thermal Response of Plasma Facing Components to Slow High Power Plasma Transients – Part I: Theory and Description of Model Capabilities," *J. Nucl. Mater.,* 244, 85 (1997). See also G. Federici, and A. R. Raffray, "RACLETTE: A Model for Evaluating the Thermal Response of Plasma Facing Components to Slow High Power Plasma Transients – Part II: Analysis of ITER Plasma Facing Components," *J. Nucl. Mater.,* 244, 101 (1997).

8. M. S. Abd El Keriem, D. P. van der Werf and F. Pleiter, "Helium-vacancy interactions in tungsten," Physical review B, Vol. 47, No. 22, 14771-14777, June 1993.

9. W. D. Wilson and R. A. Johnson, in *Interatomic Potentials and Simulation of Lattice Defects*, edited by P. C. Gehlen, J. R. Beeler and R. I. Jaffee (Plenum New York, 1972), p375.

10. S. Sharafat and N. Ghoniem, Comparison of a microstructure evolution model with experiments on irradiated vanadium," Journal of Nuclear Materials, 283-287 (2) (December 2000) 789-793.

11. N. R. Parikh, S. B. Gilliam, S. M. Gidcumb, B. K. Patnaik, J. D. Hunn, L. L. Snead, and G. P. Lamaze, "Helium Retention and Surface Blistering Characteristics of Tungsten with Regard to First Wall Conditions in an Inertial Fusion Energy Reactor," to appear in the *Journal of Nuclear Materials* (2005).

12. B. B. Cipiti and G. L. Kulcinski, "Helium and Deuterium Implantation in Tungsten at Elevated Temperatures," to appear in the *Journal of Nuclear Materials* (2005).

13. L. Snead, et al., Refractory armored first wall development, presented at the US/Japan Workshop on Laser IFE, General Atomics, San Diego, CA (March 2005), available at: http://aries.ucsd.edu/LIB/MEETINGS/0503-USJ-LIFE/program.shtml.

14. G. E. Lucas and N. Walker, "IFE Ion Threat Spectra Effects Upon Chamber Wall Materiasl, presented at the 5th High Average Power laser Program Workshop, naval Research laboratory, Washington, DC (December 2002), available at: http://aries.ucsd.edu/HAPL/MEETINGS/0212-HAPL/program.html.